applied microbiology

MDPI

Article

Development of Novel Indole and Coumarin Derivatives as Antibacterial Agents That Target Histidine Kinase in *S. aureus*

Lisha K. Poonacha [1], Rashmi Ramesh [2], Akshay Ravish [3], Arunkumar Mohan [3], Pradeep M. Uppar [3], Prashant K. Metri [3], Nanjunda Swamy Shivananju [4], Santosh L. Gaonkar [5], Shubha Gopal [2], Alexey Yu Sukhorukov [6], Vijay Pandey [7,8,9,*], Priya Babu Shubha [1,*] and Basappa Basappa [3,*]

1 Department of Studies in Chemistry, University of Mysore, Manasagangotri, Mysore 570006, India; lishakuppanda@gmail.com
2 Department of Studies in Microbiology, University of Mysore, Manasagangotri, Mysore 570006, India; rashmir97@yahoo.com (R.R.); sg@microbiology.uni-mysore.ac.in (S.G.)
3 Laboratory of Chemical Biology, Department of Studies in Organic Chemistry, University of Mysore, Manasagangotri, Mysore 570006, India; akshayrv533@gmail.com (A.R.); arunmysore3@gmail.com (A.M.); pradeepmu5@gmail.com (P.M.U.); prashant.metri@gmail.com (P.K.M.)
4 Department of Biotechnology, Technical Institutions Campus, Sri Jayachamarajendra College of Engineering, Jagadguru Sri Shivarathreeshwara University, Mysore 570006, India; nanjuchem@gmail.com
5 Department of Chemistry, Manipal Institute of Technology, Manipal University, Manipal 576104, India; sl.gaonkar@manipal.edu
6 N.D. Zelinsky Institute of Organic Chemistry, Leninsky Prospect, Moscow 119991, Russia; a.yu.sukhorukov@gmail.com
7 Shenzhen Bay Laboratory, Shenzhen 518055, China
8 Tsinghua Berkeley Shenzhen Institute, Tsinghua Shenzhen International Graduate School, Tsinghua University, Shenzhen 518055, China
9 Institute of Biopharmaceutical and Health Engineering, Tsinghua Shenzhen International Graduate School, Tsinghua University, Shenzhen 518055, China
* Correspondence: vijay.pandey@sz.tsinghua.edu.cn (V.P.); priyabs_chem@yahoo.com (P.B.S.); salundibasappa@gmail.com (B.B.)

Abstract: Heterocyclic compounds can specifically regulate bacterial development by targeting specific bacterial enzymes and metabolic pathways. The ESKAPE pathogens are multidrug-resistant and cause nosocomial infections, which is one of the greatest challenges in clinical practice. The search for novel agents to combat resistant bacteria has become one of the most important areas of antibacterial research today. Heterocyclic compounds offer a valuable strategy in the fight against resistance as they can be designed to interact with bacterial targets that are less prone to developing resistance mechanisms. Bacterial histidine kinases (HKs), which are a component of two-component bacterial systems, are a promising target for new antibacterial compounds. We have designed and synthesized novel indole derivatives as antibacterial agents. Among the series, indole-coumarin (**4b**) and bisindole (**4e**) have shown the best inhibitory activity against *S. aureus*. Further, in silico docking studies show that compounds **4b** and **4e** could target histidine kinases in bacteria.

Keywords: indole; coumarin; Suzuki coupling; histidine kinase; AutoDock

check for updates

Citation: Poonacha, L.K.; Ramesh, R.; Ravish, A.; Mohan, A.; Uppar, P.M.; Metri, P.K.; Shivananju, N.S.; Gaonkar, S.L.; Gopal, S.; Sukhorukov, A.Y.; et al. Development of Novel Indole and Coumarin Derivatives as Antibacterial Agents That Target Histidine Kinase in *S. aureus*. *Appl. Microbiol.* **2023**, *3*, 1214–1228. https://doi.org/10.3390/applmicrobiol3040084

Academic Editors: Mark G. Moloney and Sónia Silva

Received: 16 September 2023
Revised: 10 October 2023
Accepted: 11 October 2023
Published: 17 October 2023

1. Introduction

Heterocyclic compounds have broad-spectrum antibacterial activity and can target a variety of bacterial infections [1,2]. Heterocyclic compounds can specifically regulate bacterial development while causing little harm to human cells by targeting specific bacterial enzymes and metabolic pathways. Since penicillin's discovery as an antibiotic by Alexander Fleming, the advantages of this "miracle drug" have been employed to treat infectious illnesses [3]. Later, a great number of small molecules were successfully synthesized for the treatment of bacterial infections [4]. Chemists have developed structure-based drug designs that concentrate on certain pathways [5]. Virtual docking, which permits in

silico screening, can be utilized for the lead optimization of previously developed drug motifs [6,7]. Furthermore, de novo processes generate novel chemotypes for pharmaceutical compounds [8,9]. Several discoveries have been made based on natural products, such as teixobactin [10], acyldepsipeptides [11], and arylomycins [12], for antibiotics. Ciprofloxacin is a fluoroquinolone-based antibiotic used to treat a number of bacterial infections, and various reports describe bacterial resistance mechanisms to ciprofloxacin and novel techniques to improve its efficacy [13,14]. Almost all the marketed antibiotics target cell wall biosynthesis, DNA synthesis or protein biosynthesis and membrane integrity, all of which have already been counteracted via numerous resistance mechanisms [15,16].

Among many other bacteria, the ESKAPE pathogens (*Enterococcus faecalis*, *Staphylococcus aureus*, *Klebsiella pneumoniae*, *Acinetobacter baumannii*, *Pseudomonas aeruginosa*, and *Enterobacter cloacae*) are multidrug-resistant and cause nosocomial infections, which is one of the greatest challenges in clinical practice. The effects include high mortality and morbidity rates, placing a significant burden on healthcare systems [17,18]. Understanding the resistance mechanisms of these bacteria is essential for the development of novel antibacterial agents to combat infections. There is a range of antimicrobial resistance mechanisms used by ESKAPE pathogens, including enzymatic inactivation, modification of the drug target site, changing cell permeability through porin loss, an increase in the expression of efflux pumps, and mechanical protection provided by biofilm formation [19]. Thus, the search for novel agents for resistant bacteria has become one of the most important areas of antibacterial research today.

Bacterial histidine kinases (HKs), which are a component of two-component bacterial systems, are a promising target for new antibacterial compounds [20]. The histidine kinase protein is made up of two primary domains, a catalytic domain and a sensory domain, which are each responsible for detecting different signals or stimuli in the cell's environment, such as changes in temperature, osmolarity and pH or the presence of chemicals. On the other hand, the catalytic domain has kinase activity [21,22].

When histidine kinase is activated, it goes through a process called autophosphorylation, in which a phosphate group from ATP is transferred to a particular histidine residue inside the protein. The kinase domain is activated by this phosphorylation process, enabling it to work as a kinase enzyme [23,24]. The phosphorylated histidine residue is then transferred by the activated histidine kinase to a response regulator protein, which is normally found in the cytoplasm. This phosphorylation of the response regulator stimulates a series of subsequent signaling events that cause a cellular response, modulate gene expression and have an impact on cellular functions like adaptation to changing environmental conditions, metabolism regulation and cell division coordination [25,26].

Targeting histidine kinases is a promising approach to interfering with bacterial signaling pathways and disrupting critical processes required for bacterial survival and pathogenicity [27,28]. The evidence currently available suggests that various two-component systems and their related histidine kinases play distinct roles in the regulation of the critical bacterial life processes [29,30].

Heterocyclic compounds offer a valuable strategy in the fight against resistance as they can be designed to interact with bacterial targets that are less prone to developing resistance mechanisms. Isothiazolone and imidazolium salt are well-known inhibitors of histidine kinases [31]. Since the late 1940s, bacitracin, a polypeptide antibiotic made by the bacteria *Bacillus licheniformis* and *Bacillus subtilis*, has been used in clinical settings to treat staphylococcal infections, including those caused by *S. aureus*. Bacitracin inhibits cell wall production by binding to undecaprenyl pyrophosphate, and it has been effective when combined with other antibiotics to be used as a topical medication [32,33]. Daptomycin (DAP) is a lipopeptide antibiotic that has excellent antibacterial activity against most of the clinically significant Gram-positive bacteria [34]. Vancomycin is a branched, tricyclic, glycosylated peptide that was first isolated from the soil bacterium *Streptomyces orientalis* in 1956, and it is effective against Gram-positive microorganisms [35]. Luteolin and tetracycline are flavonoid compounds that are used as antibiotics [36,37].

Coumarin derivatives such as G4 poloxamer nanoparticles loaded with bioactive coumarin were evaluated for the inhibition of *S. aureus* [38], and coumarins extracted from the roots of *Ferulago campestris* showed potent antibacterial activity [39]. Synthetic coumarin derivatives like coumarin aminophosphonates [40] and various coumarin derivatives [41] have been reported for the inhibition of *S. aureus*.

Novobiocin and armillarisin A are well-known coumarin-containing antibiotics [42–45]. Many of the small molecules containing coumarin analogs, such as coumarin-triazoles (1) [46], coumarin-pyrazole (2) [47], pyranocoumarin and coumarin−sulphonamide hybrids (3) [48] and 3-amidocoumarins (4) [49], are found to inhibit *S. aureus* (Figure 1). Indoles play a vital role in antibacterial drug discovery [50], and verruculogen and tryprostatins A are commonly used antibiotics having indole motifs [51]. Indole diketopiperazine alkaloids (5) [52], benzothiophene–indole hybrids (6) [53] and deoxyribofuranosyl indoles (7) [54] are some of the reported indole derivatives that serve as inhibitors of *S. aureus*.

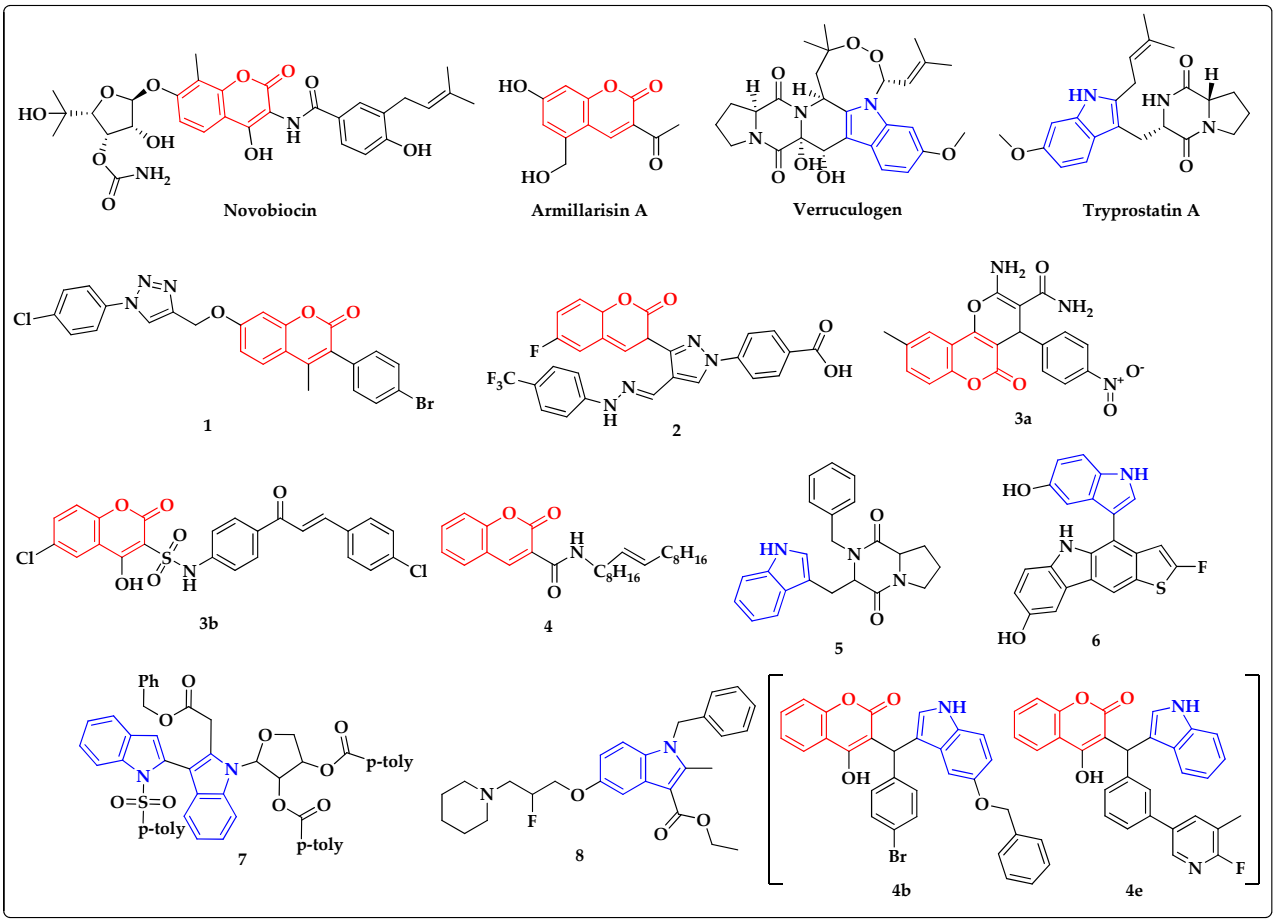

Figure 1. Reported antibacterial and histidine kinase inhibitors containing coumarin (red) and indole (blue) motifs.

Given the major task of developing small molecules containing coumarin and indoles, we have developed novel bisindoles and heterodimers of indole-clubbed coumarin analogs that are active against *S. aureus*. Further, in silico docking analysis showed that compounds **4b** and **4e** can target histidine kinases in bacteria.

2. Materials and Methods

2.1. Chemistry

The headway of the response was distinguished utilizing thin layer chromatography (TLC). Analytical TLC was performed on precoated Merck silica gel 60 F254 plates involving ethyl acetate and hexane as eluents, and spots were recognized under UV light. ^{1}H

NMR and ^{13}C NMR spectra were recorded on an Agilent NMR instrument in DMSO solvent. Chemical shifts were expressed in ppm comparative with TMS. Mass spectra were recorded on an Agilent LC-MS. All solvents and reagents were monetarily accessible and of reagent grade.

2.1.1. General Procedure for Synthesis of Indole Derivatives **4**(**a**–**m**)

A mixture of aryl aldehyde (**1**) (1 mmol), substituted indoles (**2**) (1 mmol), substituted coumarin (**3**) (1 mmol) and glycine was stirred in water:chloroform (1:1) at 70 °C for about 12 h (Table 1). Further, the reaction mass was extracted to an ethyl acetate (25 mL × 3) layer, and the solvent was removed under reduced pressure. The crude products were purified through the column chromatography technique to obtain the desired compounds **4**(**a**–**m**). The novel compounds were confirmed by ^{1}H, ^{13}C NMR and mass spectroscopy (Supplementary file contains spectral data of newly synthesized compounds).

Table 1. Conditions of reaction.

Entry	Catalyst	Solvent	Time (h)	Yield (%)
1	Nano Fe_2O_3	Ethanol	12	50
2	-	Water/Chloroform	12	73
3	Glycine	Water/Chloroform	12	92
4	I_2	DMSO	12	Not formed

2.1.2. 3-((4-bromophenyl)(1-methyl-1H-indol-3-yl)methyl)-4-hydroxy-2H-chromen-2-one (**4a**)

^{1}H NMR (400 MHz, $CDCl_3$) δ 7.65 (dd, *J* = 8.0, 1.0 Hz, 1H), 7.49 (dd, *J* = 8.6, 2.5 Hz, 4H), 7.34 (d, *J* = 1.9 Hz, 2H), 7.32 (s, 2H), 7.29 (s, 1H), 7.25–7.20 (m, 2H), 7.10 (dd, *J* = 10.9, 3.9 Hz, 1H), 6.53 (s, 1H), 5.95 (s, 1H), 3.75 (s, 3H); ^{13}C NMR (100 MHz, $CDCL_3$) δ 163.81, 162.70, 153.56, 140.21, 138.71, 132.78, 132.67, 130.74, 129.03, 127.30, 124.49, 124.08, 123.78, 121.73, 120.97, 120.06, 117.07, 116.32, 114.60, 110.39, 105.75, 39.61, 33.17; calculated mass for $C_{25}H_{18}BrNO_3$ = 459.05; obtained mass = 460.79.

2.1.3. 3-((5-(benzyloxy)-1H-indol-3-yl)(4-bromophenyl)methyl)-4-hydroxy-2H-chromen-2-one (**4b**)

^{1}H NMR (400 MHz, $CDCl_3$) δ 8.25 (s, 1H), 7.56 (dd, *J* = 7.9, 1.4 Hz, 1H), 7.50–7.45 (m, 1H), 7.39 (d, *J* = 8.4 Hz, 2H), 7.26 (d, *J* = 8.4 Hz, 5H), 7.21 (d, *J* = 2.7 Hz, 2H), 7.17–7.12 (m, 4H), 7.03 (t, *J* = 7.4 Hz, 1H), 6.93 (dd, *J* = 8.9, 2.3 Hz, 1H), 6.84 (d, *J* = 2.1 Hz, 1H), 6.56 (s, 1H), 5.81 (s, 1H); ^{13}C NMR (100 MHz, $CDCl_3$) δ 163.86, 162.80, 154.49, 153.56, 140.08, 137.78, 132.92, 132.81, 132.67, 130.70, 129.04, 128.32, 127.94, 127.21, 125.05, 124.53, 123.87, 121.76, 117.11, 116.31, 116.07, 115.68, 113.15, 105.24, 102.85, 71.02, 39.62; calculated mass for $C_{31}H_{22}BrNO_4$ = 552.42; observed mass = 552.14.

2.1.4. 3,3′-((4-bromophenyl) methylene) bis(2-methyl-1H-indole) (**4c**)

^{1}H NMR (400 MHz, $CDCl_3$) δ 5.89 (s, 1H), 6.64–6.66 (m, 2H), 7.03–7.07 (m, 2H), 7.19–7.23 (m, 2H), 7.26–7.31 (m, 4H), 7.36–7.40 (m, 4H), 7.92 (s, 2H), 2.35 (s, 6H); ^{13}C NMR (100 MHz, $CDCl_3$) δ 39.64, 111.04, 111.13, 119.21, 119.25, 119.38, 119.74, 119.83, 119.95, 121.94, 122.09, 123.61, 126.91, 128.23, 128.38, 128.74, 130.09, 131.81, 136.72, 142.59, 12.47.

2.1.5. 3-((3-(6-fluoro-5-methylpyridin-3-yl)phenyl)(1H-indol-3-yl)methyl)-4-hydroxy-7-meth-oxy-2H-chromen-2-one (**4d**)

^{1}H NMR (400 MHz, DMSO) δ 10.95 (s, 1H), 8.21 (s, 1H), 8.03 (dd, *J* = 9.6, 1.7 Hz, 1H), 7.98 (d, *J* = 9.6 Hz, 1H), 7.65 (s, 1H), 7.42–7.40 (m, 4H), 7.37 (d, *J* = 8.1 Hz, 2H), 7.16 (d, *J* = 1.9 Hz, 1H), 7.09 (t, *J* = 7.1 Hz, 1H), 6.99 (d, *J* = 2.3 Hz, 1H), 6.97 (d, *J* = 4.0 Hz, 1H), 6.94 (d, *J* = 7.0 Hz, 1H), 6.18 (s, 1H), 3.87 (s, 3H), 2.30 (s, 3H); ^{13}C NMR (100 MHz, DMSO) δ 162.75, 161.50, 154.53, 144.41, 142.73, 142.58, 140.94, 140.88, 136.53, 135.92, 128.97, 128.66,

127.65, 127.30, 125.12, 124.91, 124.76, 121.28, 119.86, 119.53, 119.00, 118.76, 114.77, 112.19, 111.96, 109.92, 106.08, 100.83, 56.35, 37.60, 14.44; calculated mass for $C_{31}H_{23}FN_2O_4$ = 506.16; obtained mass = 507.23.

2.1.6. 3-((3-(6-fluoro-5-methylpyridin-3-yl)phenyl)(1H-indol-3-yl)methyl)-4-hydroxy-2H-chromen-2-one (**4e**)

^{1}H NMR (400 MHz, DMSO) δ 10.96 (s, 1H), 8.20 (s, 1H), 8.06 (d, *J* = 8.1 Hz, 1H), 8.02 (dd, *J* = 9.6, 1.9 Hz, 1H), 7.62 (dd, *J* = 11.2, 3.9 Hz, 3H), 7.39 (d, *J* = 7.8 Hz, 7H), 7.18 (d, *J* = 2.0 Hz, 1H), 7.08 (t, *J* = 7.4 Hz, 1H), 6.95 (t, *J* = 7.3 Hz, 1H), 6.21 (s, 1H), 2.29 (s, 3H); ^{13}C NMR (100 MHz, DMSO) δ 162.72, 162.30, 160.93, 152.69, 144.12, 140.96, 140.90, 136.53, 135.97, 132.37, 129.00, 128.65, 127.64, 127.29, 124.99, 124.85, 124.25, 123.95, 121.33, 119.86, 119.53, 118.99, 118.81, 116.78, 116.69, 114.43, 111.99, 108.79, 37.75, 14.46.

2.1.7. 3-((3-(6-chloro-5-methylpyridin-3-yl)phenyl)(1H-indol-3-yl)methyl)-4-hydroxy-2H-chromen-2-one (**4f**)

^{1}H NMR (400 MHz, DMSO) δ 10.83 (s, 1H), 8.36 (s, 1H), 8.09 (d, *J* = 67.2 Hz, 1H), 7.74 (dd, *J* = 27.9, 10.1 Hz, 3H), 7.53 (s, 2H), 7.36 (d, *J* = 17.2 Hz, 5H), 7.03 (s, 1H), 6.89 (s, 3H), 5.94 (s, 1H), 2.50 (s, 3H); ^{13}C NMR (100 MHz, DMSO) δ 166.35, 146.28, 140.84, 139.96, 137.06, 135.98, 129.96, 129.61, 129.25, 129.19, 128.51, 128.18, 127.31, 127.07, 126.78, 125.96, 125.02, 124.08, 122.48, 121.38, 119.57, 118.67, 118.39, 111.95, 51.43, 32.59, 24.14.

2.1.8. 3-((3-(6-chloro-5-methylpyridin-3-yl)phenyl)(1H-indol-3-yl)methyl)-4-hydroxy-7-methoxy-2H-chromen-2-one (**4g**)

^{1}H NMR (400 MHz, DMSO) δ 10.85 (s, 1H), 8.38 (d, *J* = 6.9 Hz, 1H), 8.02 (s, 1H), 7.79 (d, *J* = 7.4 Hz, 1H), 7.74 (s, 1H), 7.69 (d, *J* = 7.6 Hz, 1H), 7.37–7.33 (m, 4H), 7.04 (t, *J* = 7.4 Hz, 2H), 6.89 (d, *J* = 10.2 Hz, 3H), 5.96 (s, 1H), 3.40 (s, 3H), 1.89 (s, 3H); ^{13}C NMR (100 MHz, DMSO) δ 166.38, 157.66, 146.28, 140.85, 139.97, 137.07, 135.99, 129.62, 129.25, 129.19, 128.20, 127.33, 127.08, 126.79, 125.98, 125.03, 124.09, 121.39, 119.59, 118.68, 118.41, 111.96, 51.45, 32.60, 24.15.

2.1.9. 3-((3-bromophenyl)(1-methyl-1H-indol-3-yl)methyl)-4-hydroxy-7-methoxy-2H-chromen-2-one (**4h**)

^{1}H NMR (400 MHz, DMSO) δ 11.81 (s, 1H), 8.04 (s, 1H), 7.63 (s, 1H), 7.39 (d, *J* = 8.4 Hz, 5H), 7.31 (d, *J* = 0.5 Hz, 2H), 7.19 (d, *J* = 29.4 Hz, 3H), 6.97 (s, 1H), 6.10 (s, 1H), 3.83 (s, 3H), 3.76 (s, 3H); ^{13}C NMR (100 MHz, DMSO) δ 162.24, 161.15, 152.70, 146.14, 136.89, 132.53, 131.20, 130.41, 129.17, 129.11, 127.84, 127.81, 124.33, 124.03, 121.64, 121.55, 119.06, 116.74, 116.71, 113.04, 110.21, 108.34, 55.82, 37.22, 32.84.

2.1.10. 3-((3-bromophenyl)(1-methyl-1H-indol-3-yl)methyl)-4-hydroxy-2H-chromen-2-one (**4i**)

^{1}H NMR (400 MHz, DMSO) δ 11.81 (s, 1H), 8.04 (s, 1H), 7.63 (s, 1H), 7.39 (d, *J* = 8.4 Hz, 5H), 7.31 (d, *J* = 0.5 Hz, 2H), 7.19 (d, *J* = 29.4 Hz, 3H), 6.97 (s, 1H), 6.10 (s, 1H), 3.76 (s, 3H); ^{13}C NMR (100 MHz, DMSO) δ 162.24, 161.15, 152.70, 146.14, 136.89, 132.53, 131.20, 130.41, 129.17, 129.11, 127.84, 127.81, 124.33, 124.03, 121.64, 121.55, 119.06, 116.74, 116.71, 113.04, 110.21, 108.34, 37.22, 32.84; calculated mass for $C_{25}H_{18}BrNO_3$ = 459.05; obtained mass = 460.15.

2.1.11. 3-((3-(6-chloro-5-methylpyridin-3-yl)phenyl)(1-methyl-1H-indol-3-yl)methyl)-4-hydroxy-2H-chromen-2-one (**4j**)

^{1}H NMR (400 MHz, DMSO) δ 8.41 (d, *J* = 2.2 Hz, 1H), 8.05 (d, *J* = 8.1 Hz, 1H), 7.99 (d, *J* = 2.0 Hz, 1H), 7.67 (s, 1H), 7.61 (t, *J* = 7.2 Hz, 1H), 7.40 (dd, *J* = 7.9, 4.9 Hz, 5H), 7.37–7.33 (m, 3H), 7.16–7.11 (m, 2H), 6.96 (t, *J* = 7.4 Hz, 1H), 6.19 (s, 1H), 3.76 (s, 3H), 2.36 (s, 3H); ^{13}C NMR (100 MHz, DMSO) δ 162.29, 160.99, 152.70, 149.81, 145.34, 144.06, 138.50, 136.97,

136.08, 135.75, 132.57, 132.41, 129.17, 129.08, 127.93, 127.35, 125.12, 124.26, 123.97, 121.45, 119.20, 118.93, 116.77, 116.70, 113.74, 110.15, 108.63, 37.76, 32.81, 19.49.

2.1.12. 3-((4-(benzyloxy)-1H-indol-3-yl) (3-(6-chloro-5-methylpyridin-3-yl) phenyl) methyl)-4-hydroxy-2H-chromen-2-one (**4k**)

^{1}H NMR (400 MHz, DMSO) δ 8.41 (d, *J* = 2.2 Hz, 1H), 8.05 (d, *J* = 8.1 Hz, 1H), 7.99 (d, *J* = 2.0 Hz, 1H), 7.67 (s, 1H), 7.61 (t, *J* = 7.2 Hz, 1H), 7.49 (dd, *J* = 8.6, 2.5 Hz, 3H, 7.40 (dd, *J* = 7.9, 4.9 Hz, 5H), 7.37–7.33 (m, 3H), 7.25–7.20 (m, 2H) 7.16–7.11 (m, 2H), 6.96 (t, *J* = 7.4 Hz, 1H), 6.19 (s, 1H), 4.9 (s, 2H) 3.76 (s, 3H), 2.36 (s, 3H); ^{13}C NMR (100 MHz, DMSO) δ 162.29, 160.99, 152.70, 149.81, 145.34, 144.06, 138.50, 136.97, 136.08, 136.76, 135.75, 132.57, 132.41, 129.17, 129.08, 128.94, 127.93, 127.6, 127.35, 127.13, 125.12, 124.26, 123.97, 121.45, 119.20, 118.93, 116.77, 116.70, 113.74, 110.15, 108.63,70.65, 37.76, 32.81, 19.49; calculated mass for $C_{38}H_{28}ClN_2O_4$ = 598.17; obtained mass = 599.14.

2.1.13. 3-((4-(6-chloro-5-methylpyridin-3-yl)phenyl)(2-methyl-2,7a-dihydro-1H-indol-3-yl)-methyl)-4-hydroxy-2H-chromen-2-one (**4l**)

^{1}H NMR (400 MHz, DMSO) δ 10.81 (s, 1H), 8.56 (d, *J* = 2.0 Hz, 1H), 8.12 (s, 1H), 8.05 (d, *J* = 7.8 Hz, 1H), 7.64 (d, *J* = 8.3 Hz, 2H), 7.60 (d, *J* = 7.4 Hz, 1H), 7.37 (d, *J* = 8.7 Hz, 2H), 7.32 (d, *J* = 8.2 Hz, 2H), 7.22 (d, *J* = 8.2 Hz, 2H), 6.92 (t, *J* = 7.6 Hz, 1H), 6.78 (t, *J* = 7.5 Hz, 1H), 6.13 (s, 1H), 2.40 (s, 3H), 2.19 (s, 3H); ^{13}C NMR (100 MHz, DMSO) δ 162.52, 161.08, 152.60, 149.63, 145.18, 143.07, 138.22, 135.54, 135.43, 134.12, 133.33, 132.56, 132.38, 129.22, 128.80, 127.25, 126.72, 124.26, 123.81, 120.03, 119.55, 118.45, 116.73, 110.72, 110.37, 107.63, 37.76, 26.81, 19.52, 13.02.

2.1.14. 3,3′-((4-(pyrimidin-5-yl) phenyl) methylene)bis(2-methyl-1H-indole (**4m**)

^{1}H NMR (400 MHz, cdcl3) δ 9.14 (s, 1H), 8.85 (s, 2H), 7.57 (s, 1H), 7.43–7.41 (m, 3H), 7.40–7.35 (m, 4H), 7.26 (s, 2H), 7.00 (dd, *J* = 16.2, 8.3 Hz, 4H), 5.98 (s, 1H), 2.61 (s, 6H); ^{13}C NMR (100 MHz, $CDCl_3$) δ 156.88, 154.83, 135.03, 134.60, 133.72, 132.70, 131.93, 129.88, 129.24, 128.65, 128.42, 124.63, 120.76, 119.18, 119.10, 112.70, 110.13, 39.14, 12.46.

*2.2. Antibacterial Activity of Compounds **4**(**a**–**m**)*

The newly synthesized compounds were evaluated for their antibacterial activity against Gram-positive (*Staphylococcus aureus* MW2 and *Enterococcus faecalis* MTCC 439) and Gram-negative (*Klebsiella pneumonia* MTCC 661, *Acinetobacter baumannii* MTCC 1425, *Pseudomonas aeruginosa* MICC 2453 and *Enterobacter cloacae* MTCC 509) bacterial strains by the agar well diffusion method as mentioned above [19]. Briefly, trypticase soy agar (TSA), brain heart infusion agar (BHI agar) and nutrient agar (NA) (pH = 7.2–7.4) plates were used. The agar plates were then inoculated with 100 µL of the test bacteria, which were grown to 1.5 × 10^8 cfu/mL (overnight culture). The test compounds, which were dissolved at a concentration of 1 mg/mL of (1:1) ethanol:distilled water, were added to each well and the plates were incubated for 24 h at 37 °C. Ethanol:distilled water (1:1) was used as a negative control. All experiments were conducted in triplicate. Compounds with the largest zone of inhibition were selected for minimum inhibitory concentration (MIC) tests. The activity of each compound was compared with that of tetracycline as a standard.

2.3. Minimum Inhibitory Concentration (MIC) of the Active Compounds

In vitro, antibacterial activity was determined by their MIC values [55,56]. A stock solution of test compounds (1 mg/mL) was dissolved in (1:1) ethanol:distilled water as a stock solution. Further, serial broth dilution was carried out to achieve compounds ranging from 120 to 500 µg/mL in TSB broth; different concentrations of test compounds (12, 15, 18. . .50 µL) were added to a standardized suspension (~10^6 cfu/mL) of the test bacterium in a tube containing 1 mL of TSB broth and incubated for 24 h at 37 °C. The minimum inhibitory concentration (MIC) was noted by observing the growth of bacteria. The lowest concentration of the drug at which there was no visible growth was considered as the MIC.

Compounds **4b** and **4e** were further investigated for their ZOI against *S. aureus*, which was expressed as the diameter of the inhibition zone according to the agar well diffusion method. All experiments were conducted in triplicate and the values are represented as mean ± SD.

2.4. Molecular Docking Studies

The three-dimensional structure of histidine kinase was obtained from a database of protein structures (RCBS) with PDB ID: 5IS1. The protein preparation was performed using the Discovery Studio software (version 21.1.0.20298), in which initially water and heteroatoms were removed and further hydrogens were added to the protein structure and later saved in a PDB format file. The structure was then prepared for docking simulations using AutoDock4 (v4.2.6) (accessed on 23 May 2023). Later, ligand preparation was performed for compound **4b** and luteolin and used for docking simulation. The binding site of histidine kinase was identified by generating a grid in AutoDock4 having grid dimensions of 40 × 60 × 50 Å, with spacing of 1 Å for both **4b** and luteolin. The ligands were then docked into the binding site using the Lamarckian Genetic Algorithm (LGA) as the search algorithm. The docking parameters were set to a population size of 150, a maximum number of 2,500,000 energy evaluations and a mutation rate of 0.02 and crossover the rate of 0.80, and 10 docking runs were performed for compound **4b** and luteolin, respectively.

The output of the docking simulations was analyzed using the AutoDock4 Tools (ADT) [57] software. The docked complexes were also visualized using PyMOL [58]; the Discovery Studio [59] and UCSF Chimera 1.16 [60] software were used to analyze the interactions between the ligand and the protein.

3. Results

*3.1. Synthesis of Bisindoles and Heterodimers of Indole-Clubbed Coumarin Derivatives **4a–m***

Using MCR, the synthesis of the condensation products of the indole, aldehyde and coumarin was carried out in the presence of different catalysts (Scheme 1). The four-component reaction was primarily optimized between 4-bromobenzaldehyde (**1**), 4-hydroxy coumarin (**2**), 5-benzyloxyindole (**3**) and iron oxide (10 mol%) in ethanol at 70 °C for 12 h and afforded **4b** with a 50% yield (Table 1, entry 1). Further, the reaction was carried out using different solvents, like DMSO and a mixture of water:chloroform (1:1); no product was formed after 12 h of reaction time (Table 1, entry 4), whereas, in the water:chloroform mixture, the product formed with a better yield (73%) (Table 1, entry 2). The same reaction was carried out by adding a glycine catalyst, resulting in the formation of the desired product in a significant yield (92%) (Table 1, entry 3). Moreover, increasing the amount of catalyst had no effect on the percentage yield. From the above observations we have synthesized derivatives **4**(**a**–**m**) (Table 2) employing glycine as catalyst (Scheme 2) using various substituted indole, coumarin and aldehydes (Figure 2).

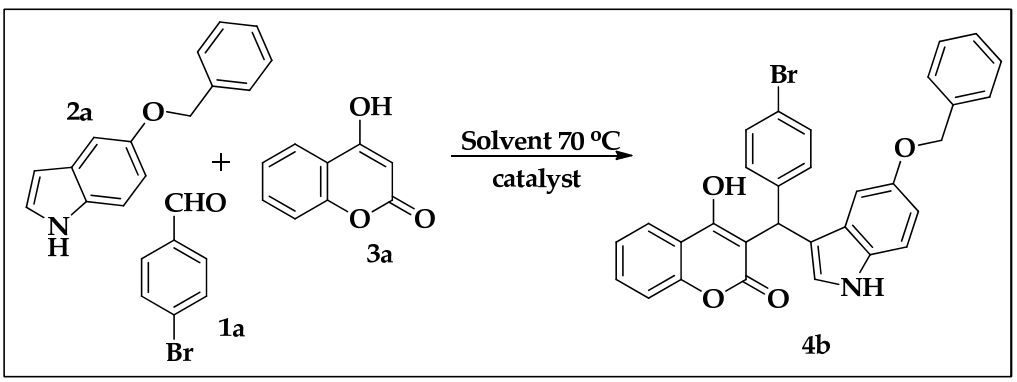

Scheme 1. Optimized reaction scheme.

Table 2. Bisindole and indole-clubbed coumarin derivatives.

Entry	Aldehydes (R_1)	Indoles (R_2)	Coumarin (R_3)
4a	**1a**	**2a**	**3a**
4b	**1a**	**2b**	**3a**
4c	**1a**	**2c**	-
4d	**1b**	**2d**	**3b**
4e	**1b**	**2d**	**3a**
4f	**1c**	**2d**	**3a**
4g	**1c**	**2d**	**3b**
4h	**1d**	**2a**	**3b**
4i	**1d**	**2a**	**3a**
4j	**1e**	**2a**	**3a**
4k	**1e**	**2e**	**3a**
4l	**1f**	**2c**	**3a**
4m	**1g**	**2c**	-

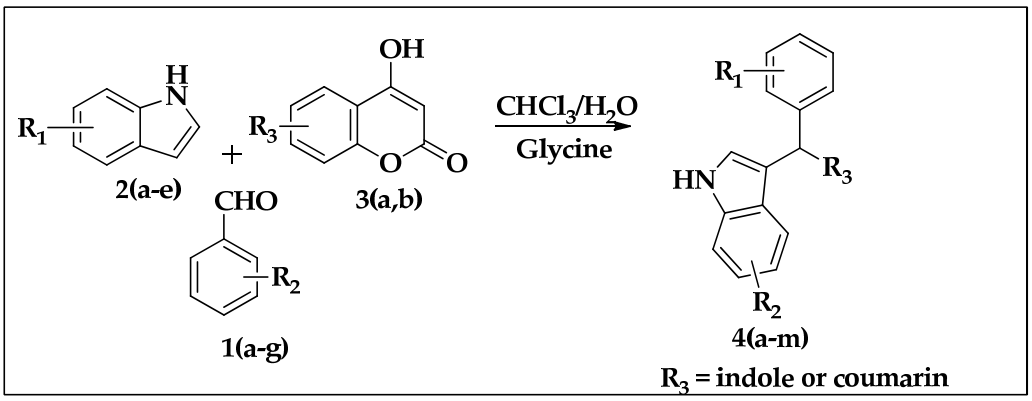

Scheme 2. Synthesis of bisindoles and heterodimers of indole-clubbed coumarin derivatives **4**(**a**–**m**).

A mixture of aryl aldehyde, substituted indoles, substituted coumarin, and glycine was stirred in water:chloroform (1:1) at 70 °C for about 12 h. After the completion of the reaction, the crude mass was extracted with ethyl acetate (25 mL × 3), distilled under high pressure, and purified through column chromatography to obtain the desired compounds **4**(**a**–**m**). The novel compounds were confirmed by ^{1}H, ^{13}C NMR, and mass spectroscopy.

3.2. Antibacterial Activity of Newly Synthesized Heterodimers of Indole-Clubbed Coumarins

All synthesized compounds were screened for antibacterial activity. As **4b** and **4e** showed activity against *S. aureus*, these compounds were checked for their minimum inhibitory concentration (MIC) and zone of inhibition (ZOI).

MIC values were evaluated at a concentration range of 120–500 µg/mL, and the results are summarized in Table 3. The MIC value of compound **4b** was 350 µg/mL and that of compound **4e** was 160 µg/mL.

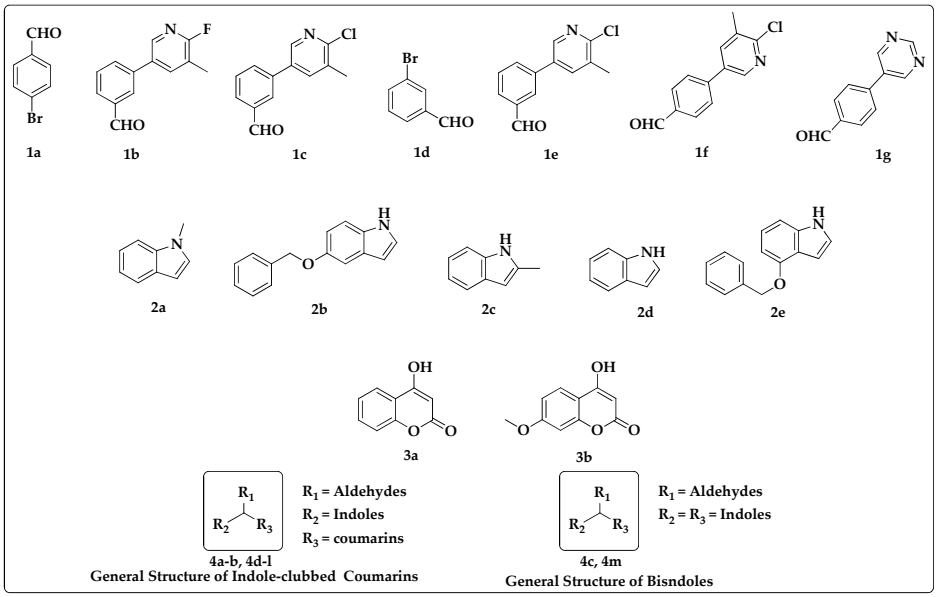

Figure 2. Substituted functional groups and general structures of bisindoles and indole-clubbed coumarin derivatives.

Table 3. Minimum inhibitory concentration (MIC) of compounds **4b** and **4e** against *S. aureus*.

Compound	MIC (μg/mL)
	S. aureus
4b (350 μg/mL)	0.256 ± 0.005
4e (160 μg/mL)	0.290 ± 0.01
Negative control (1:1) Ethanol:distilled water	0.673 ± 0.011
Positive control Tetracycline	0.206 ± 0.015

Note: MIC values evaluated at concentration range 120–500 μg/mL. The results are represented as mean ± SD.

With this MIC value for **4b** and **4e**, the ZOI was calculated by the agar well diffusion method against *S. aureus*. The ZOI of 4b was 8 mm and that of compound **4e** was 7.2 mm, as compared with tetracycline (30 μg/disc) as a positive control, showing 16.25 mm, as tabulated in Table 4.

Table 4. Zone of inhibition (ZOI) of the synthesized compounds **4b** and **4e** against *S. aureus* in mm.

Compound	Diameter of Zone of Inhibition (ZOI) (mm)
	S. aureus
4b (350 μg/mL)	8.0 mm
4e (160 μg/mL)	7.2 mm
Negative control (1:1) Ethanol:distilled water	-
Tetracycline (30 μg/disc)	16.25 mm

*3.3. In Silico Molecular Interaction Studies of Novel Compound **4b** in Inhibiting Histidine Kinase of S. aureus*

To identify the potential targets for compound **4b**, we herein used the Prediction of Activity Spectra for Substances (PASS) web tool [61], which predicts the likelihood of a compound to exhibit a particular type of biological activity based on its chemical structure. Therefore, compound **4b** in smiles format was added to the PASS web tool and we obtained the results. The PASS web tool generated a list of predicted biological activity that the compound may exhibit. From the listed targets, histidine kinase was among the top six, with Pa and Pi values of 0.421 and 0.046, and was considered the target for the bacterium *Staphylococcus aureus*.

Therefore, we retrieved the histidine kinase protein (PDB ID: 5IS1) from RCBS and later bioinformatic studies were performed using AutoDock4 tools (ADT). In this study, we used AutoDock4 to simulate the binding of a novel compound to histidine kinase, a protein involved in the regulation of bacterial virulence and antibiotic resistance. Molecular docking studies revealed that our compound **4b** had better binding affinity towards the active site of histidine kinase, showing −5.08 kcal/mol when compared to the compound luteolin, having binding affinity of −4.03 kcal/mol. The molecular interactions between compound **4b** and its target site in histidine kinase involved hydrogen bonds, with the residue GLN-73 having a bond distance of 2.35 Å. π–cation and π–anion bonds were formed with the ASN-71, ASP-96 and ASP-98 amino acid residues. Hydrophobic interactions were observed in residues ALA-72 and ILE-100. These interactions make the protein and ligand complex stable. Meanwhile, the compound luteolin exhibited the formation of hydrogen bonds with SER-127, LYS-158 and VAL-160 with bond distances of 2.26 Å, 2.24 Å, 2.93 Å and 2.45 Å, respectively. Hydrophobic interactions were formed with the residues LYS-97, LEU-126 and LYS-159 (Figure 3A,B). Luteolin and tetracycline are both members of the flavonoid class of compounds. Tetracycline, a well-known antibiotic, is structurally related to luteolin, and luteolin is studied for its potential antibacterial properties [35]. They share similar core chemical structures but differ in functional groups. This structural similarity prompted us to explore their potential similarities in inhibitory activity against histidine kinase [30]. Thus, the docking simulations predicted a better interaction between the ligand (**4b**) and the histidine kinase protein, suggesting that the compound could be an effective inhibitor of histidine kinase, and compound **4b** lies in close proximity to luteolin.

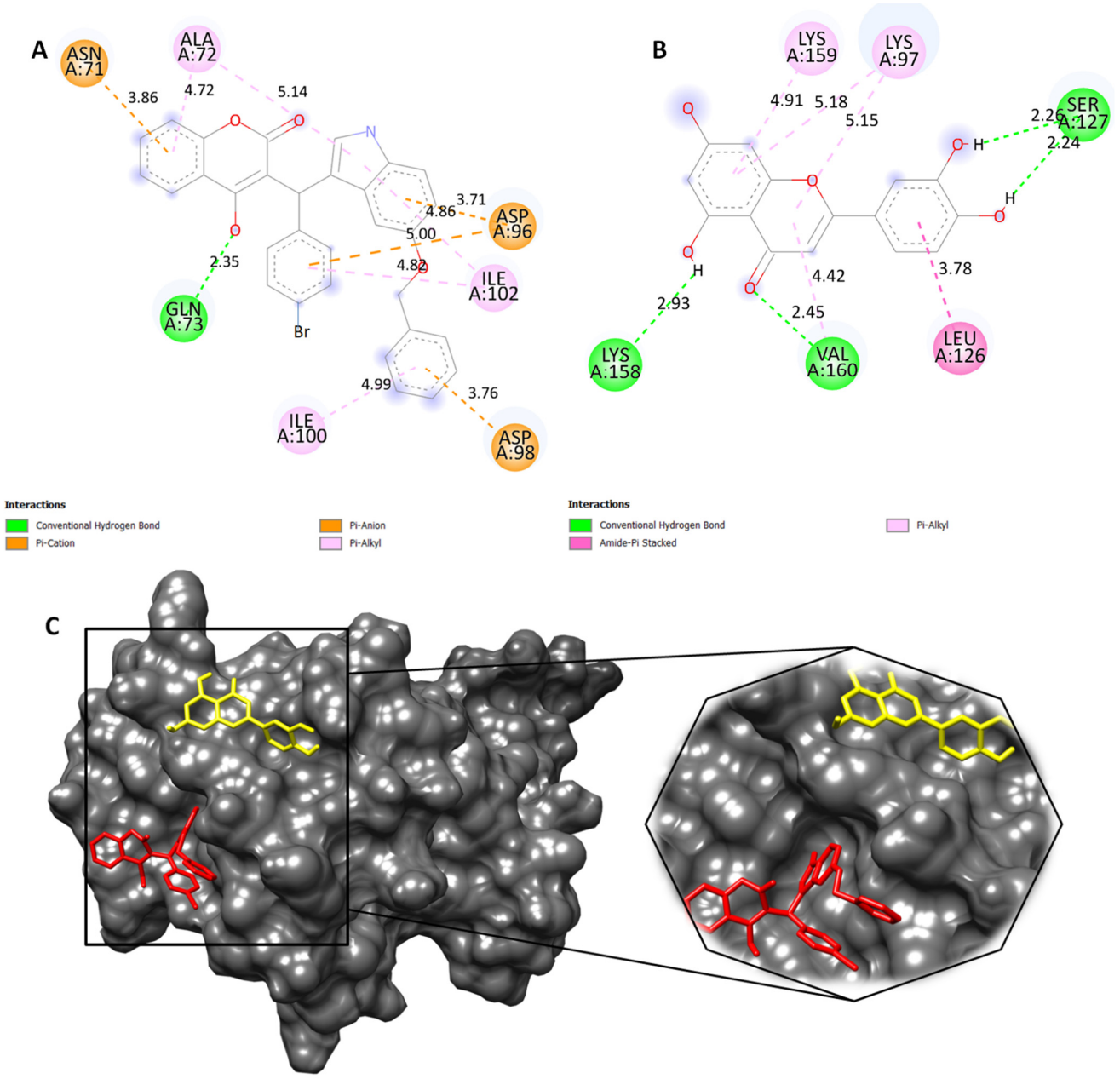

Figure 3. (**A**) Two-dimensional structure of compound **4b** (red) and (**B**) luteolin (yellow) showing molecular interactions with active site of histidine kinase. (**C**) Representation of 3D surface view of docked compounds in the groove of histidine kinase and its enlarged view for better visualization.

4. Discussion

Previously, it have been observed that the solvent and the presence of glycine played a significant part in the accomplishment of the reaction [62,63]. The outcomes propose that solvents likewise influenced the yield of compound **4b** (Table 1). After the improvement of the reaction conditions, the extent of the technique was explored with a series of substituted aromatic aldehydes, coumarins and indoles. The outcomes are collated in Table 2. Several aldehydes were synthesized by the Suzuki coupling reaction. The coupling reaction was completed by utilizing 4-bromobenzaldehyde, with various boronic acids and 1,1′-bis(diphenylphosphino)ferrocenedichloropalladium (II) as the catalyst. As observed from Table 2, the indoles having both electron-withdrawing and electron-releasing functional groups underwent effective condensation with coumarin and aldehyde in the presence of a catalytic amount of glycine in water:chloroform (1:1) at 70 °C to afford the respected

products **4**(**a**–**m**) in good yields. It appears that the electronic effects and the nature of the substituents on the indole have a slight effect on both the reaction and reaction yield. The electron-donating group at the second position of the indole increased the formation of bisindoles, rather than the heteromeric product. It was found that the reaction pathway was directed towards the formation of bisindoles, as in **4c** and **4m**. In a few of the reactions, both homomeric and heteromeric products were observed, as in **4l**.

The newly synthesized chemical compounds **4b** and **4e** exhibited promising antibacterial activity. These new data on the compounds might be helpful in their future development as novel antibacterial agents. From the present study, it may concluded that **4b** and **4e** have structural novelty and marked biological activity. This work explored on the structure and functions of biomolecules of drug development, as we previosuly reported [64–73]

5. Conclusions

Bacterial histidine kinases are components of two-component systems that serve as a promising target for new antibacterial compounds. In search of new chemical entities, we identified a new structure bearing a natural coumarin and indole rings that are attached to trigonal carbon derived from the benzene motif. The antibacterial study of the tested compounds revealed that two compounds were found to be active against pathogenic *S. aureus*, and our in silico docking study showed that the lead compound could target the histidine kinases of bacteria. In conclusion, we have identified selective antibacterial agents that could inhibit the histidine kinase of *S. aureus*.

Supplementary Materials: The following supporting information can be downloaded at: https://www.mdpi.com/article/10.3390/applmicrobiol3040084/s1, Figures in S2–S16 contain spectral data of newly synthesized compounds **4**(**a**–**m**).

Author Contributions: L.K.P., R.R., A.R., A.M., P.M.U. and P.K.M., conceptualization, methodology, formal analysis and writing; S.L.G., formal analysis; S.G., P.B.S., N.S.S., A.Y.S., V.P. and B.B., conceptualization, methodology, software, data curation, original draft, validation, writing and editing. All authors have read and agreed to the published version of the manuscript.

Funding: This work was supported by the Vision Group on Science and Technology (CESEM) and the Government of Karnataka. This research was further supported by the National Natural Science Foundation of China (82172618); the Shenzhen Key Laboratory of Innovative Oncotherapeutics (ZDSYS20200820165400003) (Shenzhen Science and Technology Innovation Commission), China; Universities Stable Funding Key Projects (WDZC20200821150704001), China; the Shenzhen Bay Laboratory, Oncotherapeutics (21310031), China; and the Overseas Research Cooperation Project (HW2020008) (Tsinghua Shenzhen International Graduate School), China. L.K.P. thanks OBC Cell, University of Mysore, Mysuru, and A.R. thanks KSTEPS, DST, Govt. of Karnataka, India, for providing the fellowship.

Institutional Review Board Statement: Not applicable.

Informed Consent Statement: Not applicable.

Data Availability Statement: All data are freely available within this article.

Conflicts of Interest: The authors declare no conflict of interest.

References

1. Campbell, I.B.; Macdonald, S.J.F.; Procopiou, P.A. Medicinal Chemistry in Drug Discovery in Big Pharma: Past, Present and Future. *Drug Discov. Today* **2018**, *23*, 219–234. [CrossRef] [PubMed]
2. Aatif, M.; Raza, M.A.; Javed, K.; Nashre-ul-Islam, S.M.; Farhan, M.; Alam, M.W. Potential Nitrogen-Based Heterocyclic Compounds for Treating Infectious Diseases: A Literature Review. *Antibiotics* **2022**, *11*, 1750. [CrossRef] [PubMed]
3. Sheehan, J.C.; Logan, K.R.H. A General Synthesis of the Penicillins. *J. Am. Chem. Soc.* **1959**, *81*, 5838–5839. [CrossRef]
4. Chellat, M.F.; Raguž, L.; Riedl, R. Targeting Antibiotic Resistance. *Angew. Chem. Int. Ed.* **2016**, *55*, 6600–6626. [CrossRef] [PubMed]
5. Grillone, K.; Riillo, C.; Rocca, R.; Ascrizzi, S.; Spanò, V.; Scionti, F.; Polerà, N.; Maruca, A.; Barreca, M.; Juli, G.; et al. The New Microtubule-Targeting Agent SIX2G Induces Immunogenic Cell Death in Multiple Myeloma. *Int. J. Mol. Sci.* **2022**, *23*, 10222. [CrossRef] [PubMed]

6. Barreca, M.; Spanò, V.; Rocca, R.; Bivacqua, R.; Gualtieri, G.; Raimondi, M.V.; Gaudio, E.; Bortolozzi, R.; Manfreda, L.; Bai, R.; et al. Identification of Pyrrolo[3′,4′:3,4]Cyclohepta[1,2-d][1,2]Oxazoles as Promising New Candidates for the Treatment of Lymphomas. *Eur. J. Med. Chem.* **2023**, *254*, 115372. [CrossRef] [PubMed]
7. Lee, B.; Kim, D.G.; Lee, A.; Kim, Y.M.; Cui, L.; Kim, S.; Choi, I. Synthesis and Discovery of the First Potent Proteolysis Targeting Chimaera (PROTAC) Degrader of AIMP2-DX2 as a Lung Cancer Drug. *J. Enzym. Inhib. Med. Chem.* **2022**, *38*, 51–66. [CrossRef] [PubMed]
8. Hajduk, P.J.; Greer, J. A Decade of Fragment-Based Drug Design: Strategic Advances and Lessons Learned. *Nat. Rev. Drug Discov.* **2007**, *6*, 211–219. [CrossRef]
9. Bivacqua, R.; Barreca, M.; Spanò, V.; Raimondi, M.V.; Romeo, I.; Alcaro, S.; Andrei, G.; Barraja, P.; Montalbano, A. Insight into Non-Nucleoside Triazole-Based Systems as Viral Polymerases Inhibitors. *Eur. J. Med. Chem.* **2023**, *249*, 115136. [CrossRef]
10. Ling, L.L.; Schneider, T.; Peoples, A.J.; Spoering, A.L.; Engels, I.; Conlon, B.P.; Mueller, A.; Schäberle, T.F.; Hughes, D.E.; Epstein, S.; et al. A New Antibiotic Kills Pathogens without Detectable Resistance. *Nature* **2015**, *517*, 455–459. [CrossRef]
11. Sass, P.; Josten, M.; Famulla, K.; Schiffer, G.; Sahl, H.-G.; Hamoen, L.; Brötz-Oesterhelt, H. Antibiotic Acyldepsipeptides Activate ClpP Peptidase to Degrade the Cell Division Protein FtsZ. *Proc. Natl. Acad. Sci. USA* **2011**, *108*, 17474–17479. [CrossRef] [PubMed]
12. Smith, P.A.; Koehler, M.F.T.; Girgis, H.S.; Yan, D.; Chen, Y.; Chen, Y.; Crawford, J.J.; Durk, M.R.; Higuchi, R.I.; Kang, J.; et al. Optimized Arylomycins Are a New Class of Gram-Negative Antibiotics. *Nature* **2018**, *561*, 189–194. [CrossRef] [PubMed]
13. Shariati, A.; Arshadi, M.; Khosrojerdi, M.A.; Abedinzadeh, M.; Ganjalishahi, M.; Maleki, A.; Heidary, M.; Khoshnood, S. The Resistance Mechanisms of Bacteria against Ciprofloxacin and New Approaches for Enhancing the Efficacy of This Antibiotic. *Front. Public Health* **2022**, *10*, 1025633. [CrossRef] [PubMed]
14. Shariati, A.; Noei, M.; Chegini, Z. Bacteriophages: The Promising Therapeutic Approach for Enhancing Ciprofloxacin Efficacy against Bacterial Infection. *J. Clin. Lab. Anal.* **2023**, *37*, e24932. [CrossRef] [PubMed]
15. Lowy, F.D. *Staphylococcus aureus* Infections. *N. Engl. J. Med.* **1998**, *339*, 520–532. [CrossRef] [PubMed]
16. Zimmermann, S.; Klinger-Strobel, M.; Bohnert, J.A.; Wendler, S.; Rödel, J.; Pletz, M.W.; Löffler, B.; Tuchscherr, L. Clinically Approved Drugs Inhibit the *Staphylococcus aureus* Multidrug NorA Efflux Pump and Reduce Biofilm Formation. *Front. Microbiol.* **2019**, *10*, 2762. [CrossRef] [PubMed]
17. Santajit, S.; Indrawattana, N. Mechanisms of Antimicrobial Resistance in ESKAPE Pathogens. *BioMed Res. Int.* **2016**, *2016*, 2475067. [CrossRef] [PubMed]
18. Mulani, M.S.; Kamble, E.E.; Kumkar, S.N.; Tawre, M.S.; Pardesi, K.R. Emerging Strategies to Combat ESKAPE Pathogens in the Era of Antimicrobial Resistance: A Review. *Front. Microbiol.* **2019**, *10*, 539. [CrossRef]
19. Balouiri, M.; Sadiki, M.; Ibnsouda, S.K. Methods for in Vitro Evaluating Antimicrobial Activity: A Review. *J. Pharm. Anal.* **2016**, *6*, 71–79. [CrossRef]
20. Bem, A.E.; Velikova, N.; Pellicer, M.T.; van Baarlen, P.; Marina, A.; Wells, J.M. Bacterial Histidine Kinases as Novel Antibacterial Drug Targets. *ACS Chem. Biol.* **2014**, *10*, 213–224. [CrossRef]
21. Casino, P.; Rubio, V.; Marina, A. The Mechanism of Signal Transduction by Two-Component Systems. *Curr. Opin. Struct. Biol.* **2010**, *20*, 763–771. [CrossRef] [PubMed]
22. Kenney, L.J. How Important Is the Phosphatase Activity of Sensor Kinases? *Curr. Opin. Microbiol.* **2010**, *13*, 168–176. [CrossRef] [PubMed]
23. Stewart, R.C. Protein Histidine Kinases: Assembly of Active Sites and Their Regulation in Signaling Pathways. *Curr. Opin. Microbiol.* **2010**, *13*, 133–141. [CrossRef] [PubMed]
24. Wolanin, P.M.; Thomason, P.A.; Stock, J.B. Histidine protein kinases: Key signal transducers outside the animal kingdom. *Genome Biol.* **2002**, *3*, reviews3013.1. [CrossRef] [PubMed]
25. Dikiy, I.; Edupuganti, U.R.; Abzalimov, R.R.; Borbat, P.P.; Srivastava, M.; Freed, J.H.; Gardner, K.H. Insights into Histidine Kinase Activation Mechanisms from the Monomeric Blue Light Sensor EL346. *Proc. Natl. Acad. Sci. USA* **2019**, *116*, 4963–4972. [CrossRef] [PubMed]
26. Kenney, L.J. How Can a Histidine Kinase Respond to Mechanical Stress? *Front. Microbiol.* **2021**, *12*, 655942. [CrossRef] [PubMed]
27. Chen, H.; Yu, C.; Wu, H.; Li, G.; Li, C.; Hong, W.; Yang, X.; Wang, H.; You, X. Recent Advances in Histidine Kinase-Targeted Antimicrobial Agents. *Front. Chem.* **2022**, *10*, 866392. [CrossRef] [PubMed]
28. Vo, C.D.; Shebert, H.L.; Zikovich, S.; Dryer, R.A.; Huang, T.P.; Moran, L.J.; Cho, J.; Wassarman, D.R.; Falahee, B.E.; Young, P.D.; et al. Repurposing Hsp90 Inhibitors as Antibiotics Targeting Histidine Kinases. *Bioorganic Med. Chem. Lett.* **2017**, *27*, 5235–5244. [CrossRef]
29. Mascher, T.; Helmann, J.D.; Unden, G. Stimulus Perception in Bacterial Signal-Transducing Histidine Kinases. *Microbiol. Mol. Biol. Rev.* **2006**, *70*, 910–938. [CrossRef]
30. Singh, V.; Dhankhar, P.; Kumar, P. Bacterial Histidine Kinases as Potential Antibacterial Drug Targets. *Protein Kinase Inhib.* **2022**, *26*, 711–734. [CrossRef]
31. Roychoudhury, S.; Zielinski, N.A.; Ninfa, A.J.; Allen, N.E.; Jungheim, L.N.; Nicas, T.I.; Chakrabarty, A.M. Inhibitors of Two-Component Signal Transduction Systems: Inhibition of Alginate Gene Activation in Pseudomonas Aeruginosa. *Proc. Natl. Acad. Sci. USA* **1993**, *90*, 965–969. [CrossRef] [PubMed]
32. Johnson, B.A.; Anker, H.; Meleney, F.L. Bacitracin: A New Antibiotic Produced by a Member of the *B. subtilis* Group. *Science* **1945**, *102*, 376–377. [CrossRef] [PubMed]

33. Stone, K.J.; Strominger, J.L. Mechanism of Action of Bacitracin: Complexation with Metal Ion and C55-Isoprenyl Pyrophosphate. *Proc. Natl. Acad. Sci. USA* **1971**, *68*, 3223–3227. [CrossRef] [PubMed]
34. Ma, W.; Zhang, D.; Li, G.; Liu, J.; He, G.; Zhang, P.; Yang, L.; Zhu, H.; Xu, N.; Liang, S. Antibacterial Mechanism of Daptomycin Antibiotic against *Staphylococcus aureus* Based on a Quantitative Bacterial Proteome Analysis. *J. Proteom.* **2017**, *150*, 242–251. [CrossRef] [PubMed]
35. Dinu, V.; Lu, Y.; Weston, N.; Lithgo, R.; Coupe, H.; Channell, G.; Adams, G.G.; Torcello Gómez, A.; Sabater, C.; Mackie, A.; et al. The Antibiotic Vancomycin Induces Complexation and Aggregation of Gastrointestinal and Submaxillary Mucins. *Sci. Rep.* **2020**, *10*, 960. [CrossRef] [PubMed]
36. Shamsudin, N.F.; Ahmed, Q.U.; Mahmood, S.; Ali Shah, S.A.; Khatib, A.; Mukhtar, S.; Alsharif, M.A.; Parveen, H.; Zakaria, Z.A. Antibacterial Effects of Flavonoids and Their Structure-Activity Relationship Study: A Comparative Interpretation. *Molecules* **2022**, *27*, 1149. [CrossRef] [PubMed]
37. Advances in Clinical Chemistry | Book Series | ScienceDirect.com by Elsevier. 1 January 2023. Available online: https://www.sciencedirect.com/bookseries/advances-in-clinical-chemistry (accessed on 20 July 2023).
38. Foudah, A.I.; Alqarni, M.H.; Ross, S.A.; Alam, A.; Salkini, M.A.; Kumar, P. Site-Specific Evaluation of Bioactive Coumarin-Loaded Dendrimer G4 Nanoparticles against Methicillin Resistant *Staphylococcus aureus*. *ACS Omega* **2022**, *7*, 34990–34996. [CrossRef]
39. Basile, A.; Sorbo, S.; Spadaro, V.; Bruno, M.; Maggio, A.; Faraone, N.; Rosselli, S. Antimicrobial and Antioxidant Activities of Coumarins from the Roots of *Ferulago campestris* (Apiaceae). *Molecules* **2009**, *14*, 939–952. [CrossRef]
40. Yang, X.-C.; Zeng, C.-M.; Avula, S.R.; Peng, X.-M.; Geng, R.-X.; Zhou, C.-H. Novel Coumarin Aminophosphonates as Potential Multitargeting Antibacterial Agents against *Staphylococcus aureus*. *Eur. J. Med. Chem.* **2023**, *245*, 114891. [CrossRef]
41. Ranjan Sahoo, C.; Sahoo, J.; Mahapatra, M.; Lenka, D.; Kumar Sahu, P.; Dehury, B.; Nath Padhy, R.; Kumar Paidesetty, S. Coumarin Derivatives as Promising Antibacterial Agent(s). *Arab. J. Chem.* **2021**, *14*, 102922. [CrossRef]
42. Vickers, A.A.; Chopra, I.; O'Neill, A.J. Intrinsic Novobiocin Resistance in Staphylococcus Saprophyticus. *Antimicrob. Agents Chemother.* **2007**, *51*, 4484–4485. [CrossRef] [PubMed]
43. Walsh, T.J.; Hansen, S.L.; Tatem, B.A.; Auger, F.; Standiford, H.C. Activity of Novobiocin against Methicillin-resistant *Staphylococcus aureus*. *J. Antimicrob. Chemother.* **1985**, *15*, 435–440. [CrossRef] [PubMed]
44. Wishnow, R.M.; Strominger, J.L.; Birge, C.H.; Threnn, R.H. Biochemical Effects of Novobiocin on *Staphylococcus aureus*. *J. Bacteriol.* **1965**, *89*, 1117–1123. [CrossRef] [PubMed]
45. Kashman, Y.; Gustafson, K.R.; Fuller, R.W.; Cardellina, J.H.; McMahon, J.B.; Currens, M.J.; Buckheit, R.W.; Hughes, S.H.; Cragg, G.M.; Boyd, M.R. HIV Inhibitory Natural Products. Part 7. The Calanolides, a Novel HIV-Inhibitory Class of Coumarin Derivatives from the Tropical Rainforest Tree, *Calophyllum lanigerum*. *J. Med. Chem.* **1992**, *35*, 2735–2743. [CrossRef]
46. Dharavath, R.; Nagaraju, N.; Reddy, M.R.; Ashok, D.; Sarasija, M.; Vijjulatha, M.; Vani, T.; Jyothi, K.; Prashanthi, G. Microwave-Assisted Synthesis, Biological Evaluation and Molecular Docking Studies of New Coumarin-Based 1,2,3-Triazoles. *RSC Adv.* **2020**, *10*, 11615–11623. [CrossRef] [PubMed]
47. Alnufaie, R.; Raj KC, H.; Alsup, N.; Whitt, J.; Andrew Chambers, S.; Gilmore, D.; Alam, M.A. Synthesis and Antimicrobial Studies of Coumarin-Substituted Pyrazole Derivatives as Potent Anti *Staphylococcus aureus* Agents. *Molecules* **2020**, *25*, 2758. [CrossRef] [PubMed]
48. Alshibl, H.M.; Al-Abdullah, E.S.; Haiba, M.E.; Alkahtani, H.M.; Awad, G.E.A.; Mahmoud, A.H.; Ibrahim, B.M.M.; Bari, A.; Villinger, A. Synthesis and Evaluation of New Coumarin Derivatives as Antioxidant, Antimicrobial, and AntiInflammatory Agents. *Molecules* **2020**, *25*, 3251. [CrossRef] [PubMed]
49. Sharma, R.K.; Singh, V.; Tiwari, N.; Butcher, R.J.; Katiyar, D. Synthesis, Antimicrobial and Chitinase Inhibitory Activities of 3-Amidocoumarins. *Bioorganic Chem.* **2020**, *98*, 103700. [CrossRef]
50. Lee, J.-H.; Cho, H.S.; Kim, Y.; Kim, J.-A.; Banskota, S.; Cho, M.H.; Lee, J. Indole and 7-Benzyloxyindole Attenuate the Virulence of *Staphylococcus aureus*. *Appl. Microbiol. Biotechnol.* **2013**, *97*, 4543–4552. [CrossRef]
51. Qin, H.-L.; Liu, J.; Fang, W.-Y.; Ravindar, L.; Rakesh, K.P. Indole-Based Derivatives as Potential Antibacterial Activity against Methicillin-Resistance *Staphylococcus aureus* (MRSA). *Eur. J. Med. Chem.* **2020**, *194*, 112245. [CrossRef]
52. Jia, B.; Ma, Y.; Liu, B.; Chen, P.; Hu, Y.; Zhang, R. Synthesis, Antimicrobial Activity, Structure-Activity Relationship, and Molecular Docking Studies of Indole Diketopiperazine Alkaloids. *Front. Chem.* **2019**, *7*, 837. [CrossRef] [PubMed]
53. Seethaler, M.; Hertlein, T.; Hopke, E.; Köhling, P.; Ohlsen, K.; Lalk, M.; Hilgeroth, A. Novel Effective Fluorinated Benzothiophene-Indole Hybrid Antibacterials against *S. aureus* and MRSA Strains. *Pharmaceuticals* **2022**, *15*, 1138. [CrossRef] [PubMed]
54. Paudel, A.; Hamamoto, H.; Kobayashi, Y.; Yokoshima, S.; Fukuyama, T.; Sekimizu, K. Identification of Novel Deoxyribofuranosyl Indole Antimicrobial Agents. *J. Antibiot.* **2011**, *65*, 53–57. [CrossRef] [PubMed]
55. Andrews, J.M. Determination of Minimum Inhibitory Concentrations. *J. Antimicrob. Chemother.* **2001**, *48*, 5–16. [CrossRef] [PubMed]
56. Kowalska-Krochmal, B.; Dudek-Wicher, R. The Minimum Inhibitory Concentration of Antibiotics: Methods, Interpretation, Clinical Relevance. *Pathogens* **2021**, *10*, 165. [CrossRef] [PubMed]
57. Huey, R.; Morris, G.M.; Olson, A.J.; Goodsell, D.S. A Semiempirical Free Energy Force Field with Charge-Based Desolvation. *J. Comput. Chem.* **2007**, *28*, 1145–1152. [CrossRef] [PubMed]
58. Schrödinger, L.L.C.; DeLano, W. PyMOL. 2020. Available online: http://www.pymol.org/pymol (accessed on 23 May 2023).
59. BIOVIA Dassault Systèmes. *Discovery Studio Visualizer, 21.1.0.20298*; Dassault Systèmes: San Diego, CA, USA, 2020.

60. Pettersen, E.F.; Goddard, T.D.; Huang, C.C.; Couch, G.S.; Greenblatt, D.M.; Meng, E.C.; Ferrin, T.E. UCSF Chimera—A visualization system for exploratory research and analysis. *J. Comput. Chem.* **2004**, *25*, 1605–1612. [CrossRef]
61. Lagunin, A.; Stepanchikova, A.; Filimonov, D.; Poroikov, V. PASS: Prediction of Activity Spectra for Biologically Active Substances. *Bioinformatics* **2000**, *16*, 747–748. [CrossRef]
62. Datta, B.; Pasha, M.A. Glycine Catalyzed Convenient Synthesis of 2-Amino-4H-Chromenes in Aqueous Medium under Sonic Condition. *Ultrason. Sonochem.* **2012**, *19*, 725–728. [CrossRef]
63. Valot, L.; Maumus, M.; Montheil, T.; Martinez, J.; Noël, D.; Mehdi, A.; Subra, G. Biocompatible Glycine-Assisted Catalysis of the Sol-Gel Process: Development of Cell-Embedded Hydrogels. *ChemPlusChem* **2019**, *84*, 1720–1729. [CrossRef]
64. Sulaiman, N.B.; Mohan, C.D.; Basappa, S.; Pandey, V.; Rangappa, S.; Bharathkumar, H.; Kumar, A.P.; Lobie, P.E.; Rangappa, K.S. An azaspirane derivative suppresses growth and induces apoptosis of ER-positive and ER-negative breast cancer cells through the modulation of JAK2/STAT3 signaling pathway. *Int J Oncol.* **2016**, *49*, 1221–1229. [CrossRef]
65. Bharathkumar, H.; Mohan, C.D.; Ananda, H.; Fuchs, J.E.; Li, F.; Rangappa, S.; Surender, M.; Bulusu, K.C.; Girish, K.S.; Sethi, G.; et al. Microwave-assisted synthesis, characterization and cytotoxic studies of novel estrogen receptor α ligands towards human breast cancer cells. *Bioorg. Med. Chem. Lett.* **2015**, *25*, 1804–1807. [CrossRef] [PubMed]
66. Blanchard, V.; Chevalier, F.; Imberty, A.; Leeflang, B.R.; Basappa; Sugahara, K.; Kamerling, J.P. Conformational studies on five octasaccharides isolated from chondroitin sulfate using NMR spectroscopy and molecular modeling. *Biochemistry* **2007**, *46*, 1167–1175. [CrossRef] [PubMed]
67. Rangappa, K.S.; Basappa. New cholinesterase inhibitors: Synthesis and structure–activity relationship studies of 1,2-benzisoxazole series and novel imidazolyl-d2-isoxazolines. *J. Phys. Org. Chem.* **2005**, *18*, 773–778. [CrossRef]
68. Sebastian, A.; Pandey, V.; Mohan, C.D.; Chia, Y.T.; Rangappa, S.; Mathai, J.; Baburajeev, C.P.; Paricharak, S.; Mervin, L.H.; Bulusu, K.C.; et al. Novel Adamantanyl-Based Thiadiazolyl Pyrazoles Targeting EGFR in Triple-Negative Breast Cancer. *ACS Omega* **2016**, *1*, 1412–1424. [CrossRef] [PubMed]
69. Srinivas, V.; Mohan, C.D.; Baburajeev, C.P.; Rangappa, S.; Jagadish, S.; Fuchs, J.E.; Sukhorukov, A.Y.; Chandra; Mason, D.J.; Sharath; et al. Synthesis and characterization of novel oxazines and demonstration that they specifically target cyclooxygenase 2. *Bioorg. Med. Chem. Lett.* **2015**, *25*, 2931–2936. [CrossRef] [PubMed]
70. Basappa; Sugahara, K.; Thimmaiah, K.N.; Bid, H.K.; Houghton, P.J.; Rangappa, K.S. Anti-tumor activity of a novel HS-mimetic-vascular endothelial growth factor binding small molecule. *PLoS ONE* **2012**, *7*, e39444. [CrossRef]
71. Priya, B.S.; Swamy, S.N.; Tejesvi, M.V.; Basappa; Sarala, G.; Gaonkar, S.L.; Naveen, S.; Prasad, J.S.; Rangappa, K.S. Synthesis, characterization, antimicrobial and single crystal X-ray crystallographic studies of some new sulfonyl, 4-chloro phenoxy benzene and dibenzoazepine substituted benzamides. *Eur. J. Med. Chem.* **2006**, *41*, 1262–1270. [CrossRef]
72. Rakesh, K.S.; Jagadish, S.; Vinayaka, A.C.; Hemshekhar, M.; Paul, M.; Thushara, R.M.; Sundaram, M.S.; Swaroop, T.R.; Mohan, C.D.; Basappa; et al. A new ibuprofen derivative inhibits platelet aggregation and ROS mediated platelet apoptosis. *PLoS ONE* **2014**, *9*, e107182, Erratum in *PLoS ONE* **2014**, *9*, e114675. [CrossRef]
73. Basappa; Rangappa, K.S.; Sugahara, K. Roles of glycosaminoglycans and glycanmimetics in tumor progression and metastasis. *Glycoconj. J.* **2014**, *31*, 461–467. [CrossRef]